MIT JOINT PROGRAM
SCIENCE POLICY
GLOBAL CHANGE

Report 322
October 2017

Mid-Western U.S. Heavy Summer-Precipitation in Regional and Global Climate Models: The Impact on Model Skill and Consensus Through an Analogue Lens

Xiang Gao and C. Adam Schlosser

MIT Joint Program on the Science and Policy of Global Change combines cutting-edge scientific research with independent policy analysis to provide a solid foundation for the public and private decisions needed to mitigate and adapt to unavoidable global environmental changes. Being data-driven, the Joint Program uses extensive Earth system and economic data and models to produce quantitative analysis and predictions of the risks of climate change and the challenges of limiting human influence on the environment—essential knowledge for the international dialogue toward a global response to climate change.

To this end, the Joint Program brings together an interdisciplinary group from two established MIT research centers: the **Center for Global Change Science (CGCS)** and the **Center for Energy and Environmental Policy Research (CEEPR)**. These two centers—along with collaborators from the Marine Biology Laboratory (MBL) at Woods Hole and short- and long-term visitors—provide the united vision needed to solve global challenges.

At the heart of much of the program's work lies MIT's Integrated Global System Model. Through this integrated model, the program seeks to discover new interactions among natural and human climate system components; objectively assess uncertainty in economic and climate projections; critically and quantitatively analyze environmental management and policy proposals; understand complex connections among the many forces that will shape our future; and improve methods to model, monitor and verify greenhouse gas emissions and climatic impacts.

This reprint is intended to communicate research results and improve public understanding of global environment and energy challenges, thereby contributing to informed debate about climate change and the economic and social implications of policy alternatives.

—Ronald G. Prinn and John M. Reilly,
Joint Program Co-Directors

MIT Joint Program on the Science and Policy of Global Change

Massachusetts Institute of Technology
77 Massachusetts Ave., E19-411
Cambridge MA 02139-4307 (USA)

T (617) 253-7492 **F** (617) 253-9845
globalchange@mit.edu
http://globalchange.mit.edu/

GLOBAL CHANGE

OCTOBER 2017

Mid-Western U.S. Heavy Summer-Precipitation in Regional and Global Climate Models: The Impact on Model Skill and Consensus Through an Analogue Lens

Xiang Gao[1,2] and C. Adam Schlosser[2]

Abstract: Regional climate models (RCMs) in general can simulate the characteristics of heavy/extreme precipitation more accurately than general circulation models (GCMs) as a result of more realistic representation of topography and mesoscale processes. An analogue method of statistical downscaling, which identifies the resolved large-scale atmospheric conditions associated with heavy precipitation, is also found to produce more accurate and precise heavy precipitation frequency across a range of GCMs in the Coupled Model Intercomparison Project Phase 5 (CMIP5) than their model-simulated precipitation alone. In this study, we examine the performances of the analogue method versus direct simulation, when applied to the RCM simulations from the North American Regional Climate Change Assessment Program (NARCCAP) and GCM simulations from CMIP5, in detecting present-day and future changes in summer (JJA) heavy precipitation over the Midwestern United States. We find the performances of two analogue schemes are comparable to those of MERRA-2 assimilated and its bias-corrected precipitation in characterizing the occurrence and interannual variations of observed heavy precipitation events, all significantly improving upon MERRA assimilated precipitation. For the late twentieth-century heavy precipitation frequency, RCM precipitation improves upon the corresponding driving GCM from CMIP5 with greater accuracy yet comparable inter-model discrepancies, while both RCM- and GCM-based analogue results outperform their model-simulated precipitation counterparts in terms of accuracy and model consensus. For the projected trends in heavy precipitation frequency through the mid twenty-first century, the analogue method also manifests its superiority to direct simulation with reduced intermodel disparities, while the RCM-based analogue and its simulated precipitation do not demonstrate a salient improvement (in model consensus) over the GCM-based assessment. However, a number of caveats preclude any overall judgement, and further work—over any region of interest—should include a larger sample of GCMs and RCMs as well as ensemble simulations to comprehensively account for modeled internal variability.

1. INTRODUCTION **2**
2. DATASETS AND METHODS **3**
3. RESULTS **5**
3.1 CALIBRATION AND VALIDATION OF ANALOGUE SCHEMES 6
3.2 SIMULATED LATE 20TH CENTURY HEAVY PRECIPITATION FREQUENCY 8
3.3 PROJECTED FUTURE CHANGES IN HEAVY PRECIPITATION FREQUENCY 9
4. SUMMARY AND DISCUSSION **11**
5. REFERENCES **13**

1 Corresponding author (Email: xgao304@mit.edu).

2 Joint Program on the Science and Policy of Global Change, Massachusetts Institute of Technology, MA, USA

1. Introduction

Extreme weather events can pose serious impacts on human society and the natural environment. One of the most important consequences of the climate changes is widespread changes in the frequency and severity of intense precipitation projected over the course of this century (Dai *et al.*, 2006; Sun *et al.*, 2006; Gutowski *et al.*, 2008; DeAngelis *et al.*, 2013). However, confidence in these projections is undermined by current climate models' inability to reproduce the observed extreme precipitation statistics of the recent past. One reason for this inability is that extreme precipitation is highly localized and influenced by regional aspects, such as orography and small-scale microphysical processes (i.e. cloud/convection), which cannot be explicitly represented with the typical resolution of global climate models. Further, the parameterizations of these processes and features can also vary greatly from one climate model to another and result in significant differences in the precipitation intensity distribution (Covey *et al.*, 2000; Wilcox and Donner, 2007).

A number of efforts have been made to address these challenges. One example is increasing the horizontal resolution of a model to improve the representation of the fine-scale features and atmospheric processes. Duffy *et al.* (2003) and Iorio *et al.* (2004) showed that high-resolution simulations using the NCAR Community Climate Model version 3 produce spatial patterns of seasonal-mean precipitation that agree more closely with observed precipitation patterns than results from the same model at coarse resolution. Oiuchi *et al.* (2006) found that tropical cyclones are simulated well enough at higher resolutions to permit a direct investigation of the effect of anthropogenic climate change on these storms. Frei *et al.* (2006) showed that the European regional climate models (RCMs) are capable of representing mesoscale spatial patterns in precipitation extremes that are not resolved by GCMs in the region of the European Alps. Kharin *et al.* (2007) demonstrated that the change in horizontal resolution of one model from ~375 to ~280 km and another from ~280 to ~110 km produced a 15 % and a 40% increase in the global average of the 20-year precipitation return value, respectively. Wehner *et al.* (2010) demonstrated that horizontal resolution is a key factor in a model's ability to reproduce observed extreme precipitation over the contiguous United States. By varying the horizontal resolution of the Community Atmospheric Model version 2 (CAM2), they concluded that the coarse resolution itself is limiting the intensity of extreme events, rather than any particular model parameterization defect. Li *et al.* (2011) also demonstrated that the horizontal resolution has a stronger impact on precipitation extremes than on mean precipitation.

Other endeavors take a different approach, namely, statistical downscaling, and focus on the large-scale atmospheric circulation features associated with the regional and local-scale extremes, which has been shown to be realistically simulated and fairly convergent in comparatively low-resolution climate models used in Phases 3 and 5 of the Coupled Model Intercomparison Project (CMIP3, CMIP5) (Gutowski *et al.*, 2008; Kawazoe and Gutowski, 2013; DeAngelis *et al.*, 2013). Several studies have illustrated how model simulated atmospheric circulation features accompanying extreme events can be characterized to derive more robust quantification of their occurrence, intensity, and changes. Hewitson and Crane (2006) demonstrated that precipitation downscaled from synoptic-scale atmospheric circulation changes in multiple GCMs can provide a more consistent projection of precipitation change than the GCMs' precipitation. Grotjahn (2011) constructed a "circulation index" based on large scale upper-air variables to forecast summertime maximum surface temperatures in California Central Valley. He found that the circulation index largely reproduces time series of the observed normalized daily maximum temperatures, even for an independent period, and performs as well as a regional model driven by large scale data. More recently, Gao *et al.* (2014, 2016) developed an "analogue method" to detect the occurrence of heavy precipitation events over the United States, which employs composites to identify prevailing large-scale atmospheric conditions associated with heavy precipitation events at local scale. They found that the method, when applied to an ensemble of CMIP5 climate model simulations, produces heavy precipitation frequencies of the late 20th century that are more consistent with observations and produces their trends through the 21st century with smaller intermodel disparity than climate model-based precipitation.

Each of these methods has strengths and weaknesses. High-resolution models are able to account for local-scale feedbacks as well as maintain the physical consistency of individual variables in time and space, but the substantial computation requirement prevents their practical uses for global simulations of long time periods. Statistical downscaling techniques give a first-order response to the regional climate change that is physically consistent with the circulation and are readily implemented across a broad range of GCMs and climate change scenarios because of low computational needs, but they are not capable of incorporating local-scale feedbacks. Questions remain around the relative value of the analogue-style statistically downscaled extreme precipitation statistics *versus* that derived from RCMs, and whether RCM simulations improve the representation of such statistics compared to the coarse resolution GCMs. GCMs have a history of intercomparison studies

(CMIP3, *et al.*, 2007; CMIP5, Taylor *et al.*, 2012) and several recent initiatives have carried out similar studies for RCMs (e.g. the Prediction of Regional scenarios and Uncertainties for Defining EuropeaN Climate change risks and Effects (PRUDENCE), Christensen *et al.*, 2007; and the North American Regional Climate Change Assessment Program (NARCCAP), Mearns *et al.*, 2009). However, an evaluation of simulated extreme precipitation across model resolutions that also examines additional benefits and comparative behaviors of the statistical/analogue methods versus direct simulation would provide valuable insights on the trade-offs between model detail, computational demand, and fidelity. Therefore, in this study, we focus on the impact of model resolution on the performances of its simulated precipitation versus its analogue in quantifying the present-day heavy precipitation frequency and their projected future changes. In order to provide a congruous evaluation across the models—noting in particular that coarser grid sizes will necessarily have smaller quantitative precipitation fluxes to represent any local precipitation event—all the GCMs and RCMs are interpolated to the common grid before heavy precipitation statistics are performed. Our study has two goals: 1) explore whether the analogue method, when used with the higher-resolution atmospheric circulation dynamics from NARCCAP but regridded to the coarser grid, can result in further improvement in detecting heavy precipitation events over the use of low resolution synoptic circulations from the CMIP5 global climate models; 2) examine if a superiority of the RCM precipitation over the GCM precipitation can be preserved in terms of estimating heavy precipitation statistics, once regridded to the coarse grid. Previous studies usually assume such superiority implicitly, but efforts in demonstrating this explicitly are rare. This exercise will provide useful insights into two aspects: 1) added value of RCMs to global model data; and 2) the selection between computationally expensive high-resolution regional models versus extensively available low-resolution GCMs when assessing heavy precipitation frequency is concerned.

Section 2 describes the datasets (observations, reanalysis, NARCCAP model simulations, and CMIP5 climate model simulations) and briefly review the methodology. Section 3 presents the late 20th century heavy precipitation frequency and projected future changes estimated based on the analogue schemes and model-simulated precipitation from NARCCAP and CMIP5 models, followed by a summary in Section 4.

2. Datasets and Methods

Daily precipitation observations are obtained from the NOAA Climate Prediction Center (CPC) Unified Precipitation" dataset (Higgins *et al.*, 2000). These observations, spanning from 1948 to present and confined to the contiguous United States, are aggregated from three sources of station rain gauge reports and gridded to a 0.25°×0.25° resolution. The model representation of heavy precipitation is usually interpreted as an average over a grid cell, so this gridded dataset is the closet comparison that can be made to the models and is far superior to comparison to individual station data.

The Modern-Era Retrospective analysis for Research and Applications, Version 2 (MERRA-2) provides data beginning in 1980 at a spatial resolution of 0.625°×0.5° (Bosilovich *et al.*, 2016). In comparison with the original MERRA dataset, MERRA-2 represents the advances made in both the Goddard Earth Observing System Model, Version 5 (GEOS-5) (Molod *et al.*, 2015) and the Global Statistical Interpolation (GSI) assimilation system that enable assimilation of modern hyperspectral radiance and microwave observations, along with GPS-Radio Occultation datasets. MERRA-2 is the first long-term global reanalysis to assimilate space-based observations of aerosols and represent their interactions with other physical processes in the climate system. In this study, we use the three-dimensional 3-hourly atmospheric diagnostics on 42 pressure levels.

The NARCCAP is a coordinated multi-model numerical experiment that provides simulations generated by a set of RCMs on a common period and domain (Mearns *et al.*, 2009). Eight RCMs, which differ greatly in their parameterized subgrid processes, are integrated at 3-hourly intervals and 50-km resolutions over the conterminous United States and most of Canada. Lateral boundary conditions are specified in two different ways. We select the set of the experiments where each of the regional models is driven with lateral boundary information from selected fully coupled global climate models. The experiments span two different periods: 1968–1999 and 2038–2070. The forcing scenario for future simulations in both the global and regional climate models was SRES A2 (Nakićenović and Swart, 2000) in the CMIP3 database. Four RCMs provide all the necessary output variables to develop the analogue schemes, including the Canadian Regional Climate Model (CRCM) (Music and Caya, 2007), the Penn State/NCAR mesoscale model (MM5I) (Grell *et al.*, 1995), the Weather Research Forecasting model (Skamarock *et al.*, 2005) that used the Grell convective parameterization scheme (WRFG) (Grell and Devenyi, 2002), and the Hadley Regional Model (HRM3) (Jones *et al.*, 2004). ECP2 and RCM3 do not output vertical velocity as required by the analogue scheme. Three driving GCMs are the Coupled Global Climate Model Version 3 (CGCM3) (Flato *et al.*, 2000) developed at the Canadian Centre for Climate Modelling and Analysis, the Community Climate System Model

version 3.0 (CCSM) (Collins *et al.*, 2006) developed at the National Center for Atmospheric Research, and the Geophysical Fluid Dynamics Laboratory's global climate model named CM2 (Delworth *et al.*, 2006) (**Table 1**).

We also compile the climate model simulations from the CMIP5 historical experiment (years 1850–2005) and experiment for the twenty-first century (years 2006–2100) employing the Representative Concentration Pathways 8.5 (RCP8.5) scenario. In this study, only one ensemble member is employed from a total of 18 models that provide all the essential meteorological variables for the analogue schemes across the two experiments (Gao *et al.*, 2016). The CMIP5 models corresponding to the driving GCMs (CGCM3, CCSM3, GFDL-CM2.1) for NARCCAP are CanESM2, CCSM4, and GFDL-CM3, respectively (Table 1). CanCM4, which is a more relevant CMIP5 model corresponding to CGCM3, is not employed due to its limited output variables available. However, as shown in Chylek *et al.* (2011), the inclusion of CTEM (a dynamic vegetation and transition from CanCM4 to CanESM2) does not improve further the agreement between the observed and modeled temperature anomaly. In addition, The RCMs driven by HadCM3 are not included because HadCM3 in CMIP5 does not output all the necessary meteorological variables.

The same set of meteorological variables are assembled or derived from the MERRA-2 reanalysis, NARCCAP regional and CMIP5 climate model simulations, including 500 hPa vector winds (uv_{500}), 500 hPa vertical velocity (w_{500}), near-surface specific humidity (q_{2m}), and total precipitable water (*tpw*). These fields represent key environmental conditions during heavy precipitation development and are readily available in the output archives of most of the models involved in the various model intercomparison projects. The 3-hourly MERRA-2 atmospheric diagnostics and NARCCAP simulations are averaged into daily values. The thin-plate-spline algorithm is then employed to convert NARCCAP daily data of various projections to a regular 0.5°×0.5° lon-lat grid. All the daily fields, including the precipitation observation as well as the precipitation and meteorological fields from MERRA-2 reanalysis, NARCCAP RCMs, and CMIP5 climate models, are further regridded to the common 2.5°×2° resolution through conservative regridding as suggested by Chen and Knutson (2008). We regrid the higher resolution RCM and lower resolution GCM simulations to the common grid to examine the effect of the models' native horizontal resolution for regridding on the performances of two distinctive analyses (model-based precipitation versus analogue schemes) in quantifying heavy precipitation frequency and its change.

Table 1. NARCCAP regional models selected in this study, corresponding driving climate models, and model counterparts in CMIP5. Also listed in the parenthesis are main components of coupled global climate models in the form of component name followed by version number as well as the specific ensemble run employed. The italic texts indicate the model components with update.

		NARCCAP		
CMIP5		**Driving Model (CMIP3)**		**RCM (~50km)**
Model / Run	**Resolution**	**Model / Run**	**Resolution**	
CCSM4 run6	**288x192**	**CCSM3** run5	**256x128**	CRCM, WRFG, MM5I
CAM4 [a1]		CAM3 [a1]		
POP2 [a2]		POP1.4.3 [a2]		
CICE4 [a3]		CSIM5 [a4]		
CLM3.5 [a5]		CLM3 [a5]		
CanESM2 [b1] run1	**128x64**	**CGCM3** [b2] run4	**96x48**	CRCM, WRFG
CanCM4 [b3]		CanCM3 [b3]		
CTEM [b4]				
GFDL-CM3 run1	**144x90**	**GFDL-CM2.1** run2-historical, run1-future	**144x90**	HRM3
AM3 [c1]		AM2 [c1]		
LM3 [c2]		LM2 [c2]		
MOM4 [c3]		MOM4 [c3]		
SIS [c4]		SIS [c4]		

[a] Source: Gent *et al.* (2011)
[1] Community Atmosphere Model
[2] Parallel Ocean Program
[3] Community Ice Code
[4] Community Sea Ice Model
[5] Community Land Model
[b] Source: Chylek *et al.* (2011)
[1] Canadian Earth System Model
[2] Coupled Global Climate Model
[3] Canadian Centre for Climate Modeling and Analysis (CCCma) Coupled Climate Model
[4] Canadian Terrestrial Ecosystem Model
[c] Source: Griffies *et al.* (2011)
[1] Atmospheric component
[2] Land component
[3] Ocean component
[4] Sea ice component

The overlap period is 1 January 1980–31 December 1998 among the CPC observations (1948–present), MERRA-2 reanalysis (1980–present), NARCCAP experiment (1968–1999), and the CMIP5 historical experiment (1850–2005). At each grid cell, we convert the meteorological fields of each data source to normalized anomalies based on their respective seasonal climatological mean and standard deviation of this 19-yr period. The same seasonal climatological means and standard deviations are also employed to calculate the normalized anomalies for the meteorological fields of MERRA-2 reanalysis from 1999 to 2014, NARCCAP future experiment from 2038 to 2070, and CMIP5 RCP8.5 experiment from 2038 to 2070. The projected changes in heavy precipitation frequency for both NARCCAP and CMIP5 experiments focus on two 19-yr periods centered at the years 2050 (2041–2059) and 2060 (2051–2069), respectively. For both model-based precipitation and the analogue schemes of NARCCAP and CMIP5, the change of each model is calculated relative to its respective seasonal heavy precipitation frequency from 1980 to 1999 and expressed as number of events per year.

We use the CPC observed precipitation to identify the heavy precipitation events. A heavy precipitation event at any grid cell of 2.5°×2° is its daily amount exceeding the 95th percentile of all rain days (> 1 mm) at that grid cell during a specific period (season). The 95th percentile of the observed precipitation distribution based on contemporary climate (1980–1998) is used to extract the heavy precipitation events for MERRA-2 reanalysis from 1980 to 2014 as well as for NARCCAP and CMIP5 of historical experiment from 1980 to 1998 and future experiment from 2041 to 2069. Gao *et al.* (2016) found that precipitation generated by the AGCM within the cycling MERRA data assimilation system (hereinafter referred to as *MERRA_P*) significantly underestimated the occurrence and interannual variations of observed heavy precipitation events in the MWST. Here we compare *MERRA_P* with precipitation generated by the AGCM within the cycling MERRA-2 data assimilation system (hereinafter referred to as *MERRA2_P*) and bias-corrected MERRA-2 precipitation seen by the land surface and aerosol wet deposition over land and ocean (hereinafter referred to as *MERRA2_Pc*). These three products correspond to MERRA, M2AGCM, and M2CORR in Reichle *et al.* (2017), respectively. We then aggregate all extracted events at all data grid cells within the region of our interest from each data source separately. The MERRA-2 reanalysis is employed to construct the large-scale composites of atmospheric patterns associated with identified heavy precipitation events. The MERRA-2 reanalysis large-scale atmospheric fields from 1980 to 1998 will be used to develop and calibrate the analogue schemes, and from 1999 to 2014 to validate them.

Here we examine two analogue schemes based on 500 hPa horizontal and vertical winds (uvw_{500}) and each of two moisture variables, namely, near-surface specific humidity (q_{2m}) and total-column precipitable water (tpw). The corresponding analogue schemes are hereinafter referred to as $uvw_{500}q_{2m}$ and $uvw_{500}tpw$, respectively. The analogue scheme $uvw_{500}tpw_{500}$ (constructed with total precipitable water to 500 hPa) is not included due to the similar results to those of $uvw_{500}tpw$ (Gao *et al.*, 2016). Our main intent is to examine how the CMIP5 GCMs and NARCCAP RCMs with the same driving GCM, when regridded to the common grid, perform in detecting the occurrence of heavy precipitation events under contemporary climate and quantifying its change as climate warms—based on prevailing large-scale physical mechanisms *versus* more conventional model-simulated precipitation, in comparison with observations. We are also interested in how the use of MERRA-2 atmospheric synoptic conditions to construct the analogue compares with the MERRA counterparts as used in Gao *et al.* (2016).

3. Results

We focus our analyses on one of the two regions analyzed in our previous work (Gao *et al.*, 2016)—the summer season (June-August, JJA) of the Midwestern United States (MWST). Based on our earlier discussion and given that summer-season precipitation over this region is strongly influenced by convective processes, this should presumably provide a strong testbed and cater to the higher resolution grid from the NARCCAP RCMs. We use the same region as defined in Gao *et al.* (2016), bounded by 39°–45°N and 98.75°–88.75°W at the 2.5°×2° resolution (20 grid cells shown as red rectangle in Figure 1a). **Figure 1** shows the composites as standardized anomalies by averaging the MERRA-2 reanalysis across the extracted 400 heavy precipitation events from the observation of 1980–1998 at 2.5°×2°. Although the standardized anomalies of all the meteorological fields are not strong, we see heavy precipitation occurring with the presence of lower heights to the west and higher heights to the east of the analysis region as well as the transport of warm, moist air from the Gulf of Mexico north-northeastward across the north-central United States (Figure 1a). The composite exhibits characteristics of the "Maya Express" that fetches moisture from the subtropics or tropics, with the origins of this moisture plume possibly extending farther south and east toward the Caribbean Sea. Also evident are moister air and stronger upward motion centered on the study region (Figure 1b). These features represent the preferred synoptic conditions conducive to heavy precipitation events in this region.

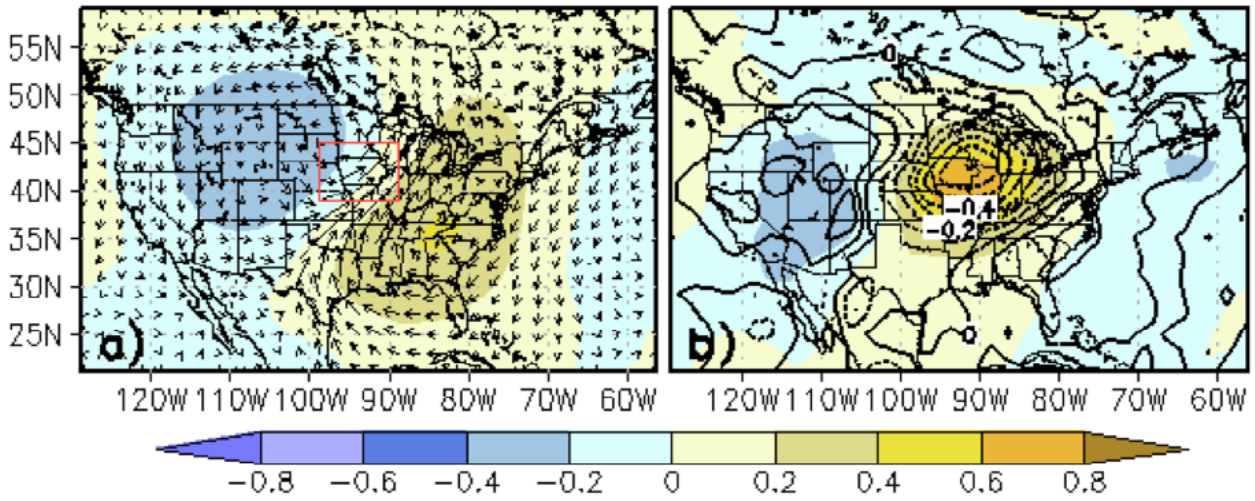

Figure 1. Composite fields as normalized anomalies for the Midwestern United States (MWST) in JJA. (a) 500-hPa geopotential height (shaded) and the vertical integrated water vapor flux vector up to 500 hPa (arrow) based on 400 heavy precipitation events at 2.5°×2°. (b) 500-hPa vertical velocity (contour, w_{500}) and total precipitable water (*tpw*; shaded). The red rectangles depict our study regions.

We follow the same procedure as described in Gao *et al.* (2016) to develop, calibrate and validate the analogue schemes and will briefly state it here. Two metrics, the "hotspot" and the spatial anomaly correlation coefficient (SACC), are employed to characterize the matching to the distinct synoptic conditions conducive to heavy precipitation events shown in composites. We use these metrics to quantify the degree of consistency between the composites and daily MERRA-2 atmospheric fields of 1980–1998. Five performance measures that are commonly used in a "confusion matrix" for binary classification are adopted, including True Positive Rate (TPR), False Positive Rate (FPR), Accuracy (ACC, the ratio of combined true positives and true negatives to total population), Precision (PPV, the proportion of correctly identified events to the total identified heavy events), and F1 score (the harmonic mean of PPV and TPR). The optimal cutoff values for the number of hotspots and thresholds for SACC are chosen to produce the observed number of heavy precipitation events (equal to the sum of true positives and false positives) with the best TPR. The established detection criteria will be applied to the 1999–2014 MERRA-2 reanalysis as well as the CMIP5 and NARCCAP historical and future model-simulated daily meteorological conditions to obtain analogue-based heavy precipitation events by judging their similarities against the constructed composites. We then compare the results of analogue schemes with the heavy precipitation events identified from the observations, three MERRA precipitation products, the CMIP5 and NARCCAP model precipitation (all at 2.5°×2° resolution).

3.1 Calibration and Validation of Analogue Schemes

Table 2 shows performance measures of two analogue schemes and three MERRA precipitation products in detecting heavy precipitation events during calibration (1980–1998) and validation (1999–2014) periods. During the calibration period, *MERRA_P* and *MERRA2_Pc* underestimate the number of heavy precipitation events, while *MERRA2_P* overestimates the events. These features are consistent with their relative magnitude differences as shown in Fig. 3b and d of Reichle *et al.* (2017). The overestimated number of events by *MERRA2_P*, as expected, leads to the highest TPR (75%), but usually at the expense of the highest FPR (19%) as well. The strong underestimation by *MERRA_P* presents the opposite case to that of *MERRA2_P* with the lowest TPR (23%) and FPR (2%). The *MERRA2_Pc* lies in between with TPR and FPR being 49% and 5%, respectively. Two analogue schemes exhibit fairly similar performances and show lower TPR and FPR than *MERRA2_P*, but higher TPR and FPR than *MERRA2_Pc*. We found ACC fairly insensitive with small changes across all five schemes, likely attributed to our unbalanced dataset with non-heavy events (and thus true negative) occupying the large portion. The magnitude of PPV does not follow a simple rule as it is related to how the total identified heavy events by each scheme is partitioned between correctly and falsely identified events. The magnitudes of F1 score are largely consistent with TPRs, with *MERRA2_P* and *MERRA_P* being highest and lowest, the two analogue schemes and *MERRA2_Pc* being similar and slightly lower than *MERRA2_P*. Overall, there is no single scheme

Table 2. Calibration and validation statistics with two combinations of atmospheric variables to construct analogue diagnostics. FNR and TNR are not included in the table as they can be simply derived from TPR and FPR, respectively. The red numbers indicate the total number of observed heavy precipitation events.

Scheme	TPR	FPR	ACC	PPV	F1 Score	Total Events
			1980–1998			**400**
MERRA_P	0.228	0.020	0.808	0.771	0.351	118
MERRA2_P	0.748	0.185	0.799	0.545	0.630	549
MERRA2_Pc	0.490	0.051	0.844	0.740	0.589	265
$uvw_{500}q_{2m}$	0.587	0.122	0.811	0.587	0.587	400
$uvw_{500}tpw$	0.580	0.125	0.808	0.580	0.580	400
			1999–2014			**367**
MERRA_P	0.155	0.024	0.771	0.679	0.253	84
MERRA2_P	0.681	0.167	0.796	0.576	0.624	434
MERRA2_Pc	0.466	0.066	0.817	0.701	0.560	244
$uvw_{500}q_{2m}$	0.425	0.116	0.770	0.549	0.479	284
$uvw_{500}tpw$	0.425	0.113	0.772	0.555	0.481	281

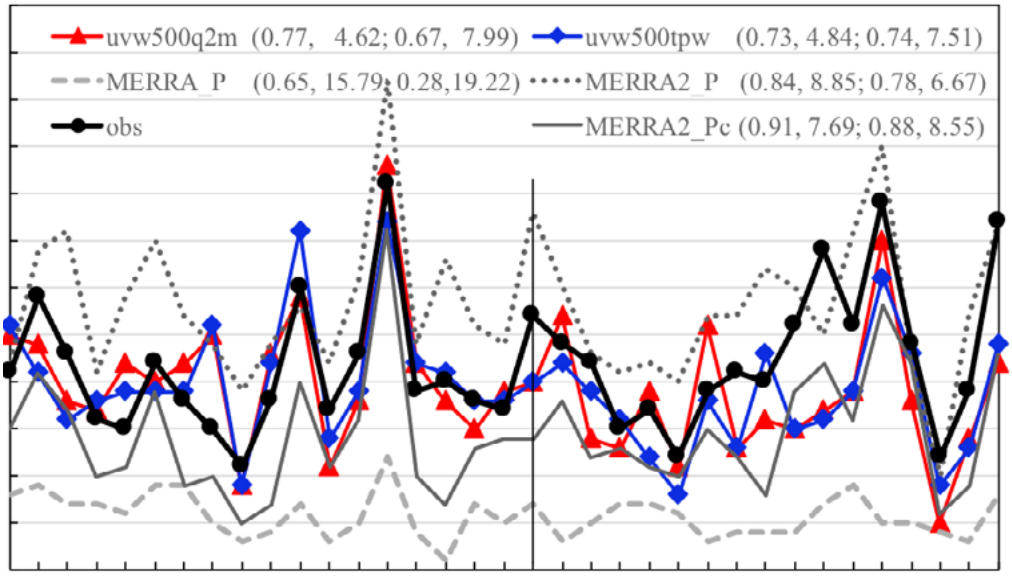

Figure 2. Comparisons of interannual variations of JJA heavy precipitation frequency obtained from analogue schemes, MERRA precipitation (*MERRA_P*), MERRA-2 (*MERRA2_P*) and MERRA-2 bias-corrected (*MERRA2_Pc*) precipitation, and the observation (obs) during the calibration (1980–1998) and validation (1999–2014) periods. Also shown in the parentheses of figure legend are temporal correlations and RMSE between various schemes and observation during two periods.

that performs consistently better than others across all the measures; however, a salient feature is the relatively poorer performance of *MERRA_P* in comparison with the other schemes. During the validation period, we see similar characteristics across various schemes except that nearly all the performance measures are worse than those during the calibration. In comparison with two MERRA-2 precipitation products, the performance degradation in the analogue schemes is stronger, particularly in TPRs and F1 scores. This is expected as the analogue schemes are evaluated to data that is independent (i.e. non-overlapping) from the training data used for tuning. Precipitation from MERRA-2, however, contains assimilated observations throughout both periods. Note that the analogue schemes tend to underestimate the number of heavy precipitation events, but not as strongly as *MERRA2_Pc*.

Figure 2 shows the performances of two analogue schemes in depicting the interannual variations of summer heavy precipitation frequency from 1980 to 1998 (calibration) and 1999 to 2014 (validation) as compared to the obser-

vations and three MERRA precipitation products. It is readily seen that *MERRA_P* significantly underestimates the number of heavy events throughout the entire 35-yr period, and the resulting temporal correlations are lower and the root-mean-square errors (RMSEs) considerably higher than all the other schemes, especially during the validation period. Two analogue schemes and MERRA-2 precipitation (*MERRA2_P* and *MERRA2_Pc*) reproduce the observed interannual variations of heavy precipitation frequencies reasonably well with comparable temporal correlations (0.7~0.9) and RMSEs (5~8 days) during both periods. More specifically, they capture to varying degrees the peaks in occurrence during 1990, 1993, 2010, and 2014 as well as years with relatively low frequency of events such as 1988, 2003, and 2012. Mostly, *MERRA2_P* tends to overestimate the number of heavy precipitation events, while *MERRA2_Pc* tends to underestimate it. The analogue schemes underestimate the observed number of events for 1998, 2005–2009 and 2014, but overestimate the 1987 number of events.

3.2 Simulated Late 20th Century Heavy Precipitation Frequency

Figure 3 displays the comparisons of the number of 1980–1998 summer heavy precipitation events obtained from the CMIP5 and NARCCAP model precipitation as well as by applying two analogue schemes to the CMIP5 and NARCCAP atmospheric synoptic conditions. Also included are the numbers of heavy precipitation events estimated from the observations and three MERRA precipitation products. The precipitation from 17 out of 18 CMIP5 models (*CMP_pr* in Figure 3) underestimates the number of heavy precipitation events. The models exhibit a varying degree of underestimation, resulting in a considerably wide interquartile range (IQR, 155 days) and inter-model spread (370 days). In contrast, the results from two analogue schemes (*CMP_uvw*$_{500}$*_tpw* and *CMP_uvw*$_{500}$*_q*$_{2m}$) produce the multi-model medians that are much more consistent with the observation as well as reduced IQRs and inter-model ranges (i.e. a stronger model consensus). The scatters of three labeled CMIP5 models clearly manifest such differences in the spread of precipitation- *versus* analogue-based results. The analogue scheme based on *tpw* slightly outperforms that based on q_{2m} with stronger model convergence.

The precipitation from GCM-driven NARCCAP ensemble (*NAR_pr* in Figure 3) also underestimates the number of heavy precipitation events. This is in agreement with Singh *et al.* (2013, Fig. S4), who reported the underestimation of summer wet extreme days in parts of central U.S. based on the five CCSM3 driven RegCM3 ensembles. However, RCMs generally improve upon the corresponding CMIP5 models, except for the CRCM driven by CCSM which shows a larger negative bias than the CCSM4 in CMIP5. Such improvement is expected and likely attributed to better resolution of the atmo-

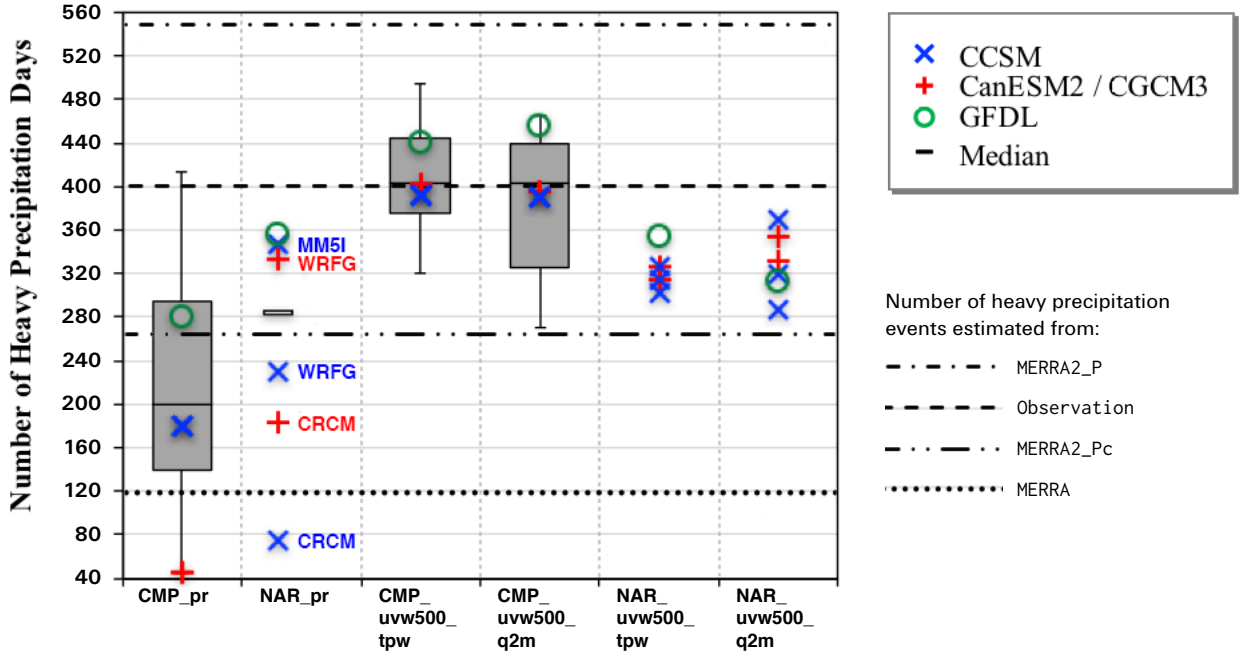

Figure 3. Comparisons of the number of summer (JJA) heavy precipitation events estimated from CMIP5 and NARCCAP model-simulated precipitation as well as analogue schemes applied to CMIP5 and NARCCAP model-simulated atmospheric synoptic conditions during the period of 1980 to 1998. The whisker plot shows the minimum, the lower and upper quartile, median, and the maximum across 18 CMIP5 models. The scatters represent NARCCAP RCMs and the corresponding driving GCMs from CMIP5.

spheric fluid dynamics, surface boundary conditions, and smaller-scale weather systems that often produce intense rainfall in mid-continent areas in the summertime at the RCMs' higher spatial resolution. The regridded coarse-resolution precipitation from RCMs seems able to preserve the features inherent in its native resolution to some extent. This is also reported by Wehner *et al.* (2010), who showed that the simulated twenty-year return values of the annual maximum daily precipitation totals are substantially lower than the observations regridded to the model's coarse native mesh. The improvement is greater for two RCMs driven by CGCM3 and MM5I driven by CCSM. However, there is no single RCM (i.e. WRFG or CRCM) driven by multiple GCMs or multiple RCMs driven by a single GCM (i.e. CCSM or CGCM3) that consistently performs better than its peers. The results that are more consistent with the observation can occur to different RCM-GCM combinations, such as HRM3-GFDL, MM5I-CCSM, and WRFG-CGCM3. We find that CRCM or WRFG driven by CGCM3 boundary conditions gives a larger number of heavy precipitation events than that driven by CCSM, while CRCM driven by two GCMs exhibits a smaller number of events. Several studies documented that CRCM driven by the reanalysis of the National Center for Environmental Prediction (NCEP-2) produces too low extreme precipitation metrics as compared to the observed and other regional model results (Fig. 2 of Wehner, 2013, Table 2 of Kawazoe and Gutowski Jr., 2013). Worthy of note is that three RCMs driven by the CCSM lead to a fairly wide range of scatter, with the number of heavy precipitation events ranging from 74 to 347, roughly comparable to the entire range by six RCM-GCM combinations and 18 CMIP5 models. Wehner (2013) also found significant variation in NARCCAP RCMs' abilities to reproduce observed 20-year return values of seasonal maximum daily precipitation rates over the contiguous United States. RCMs are well known to be very sensitive to the choice of parameterization schemes and physics packages (Christensen *et al.*, 2007). The four regional models employed here differ greatly in their formulation of subgrid scale turbulence, radiative transport, boundary layer effects and moist processes. Specifically, the moist processes, including parameterized treatments of shallow and deep convective cloud processes as well as larger scale cloud physics, are the most relevant to the precipitation simulation. Global climate models that RCMs rely on for the lateral boundary conditions adds additional uncertainty.

Two analogue schemes based on the regridded coarse-resolution RCMs slightly underestimate the heavy precipitation frequencies as well (*NAR_uvw*$_{500}$*_tpw* and *NAR_uvw*$_{500}$*_q*$_{2m}$ in Figure 3), but clearly improve upon the corresponding model precipitation with largely reduced inter-model spread and collectively more consistent frequencies with the observation. Likewise, the analogue scheme based on *tpw* marginally outperforms that based on q_{2m} with slightly smaller inter-model range (52 vs. 83 days). Different from the model precipitation, the heavy precipitation frequencies from the analogue schemes do not improve upon those from the corresponding CMIP5 models, particularly for CCSM and CanESM2. The better performances of the analogue schemes from CMIP5 models than from RCMs (driven by the previous version of GCMs) are likely attributed to the improved model physics (i.e. updated algorithms and schemes) in the newer versions of climate model components employed in CMIP5 (Gent *et al.*, 2011; Chylek *et al.*, 2011; Donner *et al.*, 2011). For example, Chylek *et al.* (2011) showed that the CanCM4 and CanESM2 simulations reproduce reasonably well the 20th century Arctic temperature anomaly, including the amplitude, the timing of the early 20th century warming, and subsequent significant cooling, while the simulations of the CMIP3 models (CanCM3 and CCSM3) cannot reproduce these features.

Overall, the analogue schemes greatly improve upon the model precipitation in terms of their assessment of late twentieth-century heavy precipitation frequency from the perspectives of both accuracy (consistencies with observation) and precision (inter-model spreads), regardless of the atmospheric synoptic conditions or precipitation chosen from the coarse-resolution GCMs or the high-resolution RCMs regridded to the coarse resolution. The performances of the analogue schemes remain fairly robust between regional and global models. The high-resolution regional models do not add much value to global model results, mostly because analogue schemes essentially rely on the synoptic atmospheric features which are well resolved at the coarse-resolution global models. Our results also suggest that current state-of-the-art regional and climate models are capable of realistically simulating the atmospheric synoptic conditions associated with heavy precipitation events with reasonable frequencies. Accordingly, the analogue schemes can provide more useful skill in detecting heavy precipitation events than corresponding model-simulated precipitation.

3.3 Projected Future Changes in Heavy Precipitation Frequency

Due to the natural chaotic behavior of the climate system, projection of future climate change based on a single realization of a single climate model cannot reproduce the great spatial heterogeneity of heavy precipitation in reality, regardless of model quality. Projected changes in heavy precipitation statistics from large ensembles of realizations are less spatially heterogeneous and should be considered in a probabilistic rather than in a deter-

ministic sense. In comparison with CMIP5, the limited ensemble size of the NARCCAP projections poses challenges in quantifying such a probabilistic interpretation, but should still provide some useful insights.

Figure 4a displays the changes in heavy precipitation frequency estimated from an ensemble of CMIP5 model precipitation and the analogue scheme $uvw_{500}tpw$ under the RCP8.5 scenario as well as the counterparts from NARCCAP under the SRESA2 scenario. The multimodel medians of both analyses from CMIP5 (*CMP_Pr_* and *CMP_A_*) indicate decreases in heavy precipitation frequency, with the drying trends of the analogue results stronger than those of precipitation. The medians of precipitation and analogue results suggest 0.3–0.6 and 2.0–2.8 fewer events per year, respectively. Previous studies also reported the projected reduction in the summer daily maximum precipitation rate or the frequency of summer wet extremes in the Midwestern U.S. in the mid- or late- 21st century (Wehner, 2013, Singh *et al.*, 2013). For both analyses, the majority of the models (50% ~ 75% or so) indicate decreases in the frequency. We see all three labeled GCMs manifest such drying trends. There are considerable uncertainties in the magnitude of change. However, the analogue scheme demonstrates reduced disagreements in the sign and magnitude of change in comparison with CMIP5 model precipitation during the same period. The distribution of projected changes ranges from decrease of 7 to increase of 5 events per year for precipitation, but from decrease of 6.5 (or 8) to increase of 3.5 (or 2) events per year for the analogue scheme.

The GCM driven RCMs (*NAR_Pr_* and *NAR_A_*) show very mixed responses. The CRCM and WRFG driven by the same GCM (CCSM or CGCM3) can have opposite signs of change in frequency for both model precipitation and analogue scheme, mostly with the drying trends for the CRCM but wetting trends for the WRFG, although the trends are sometimes relatively weak.

The same RCM (CRCM or WRFG) driven by CCSM generally shows stronger decreases (or weaker increases) than that driven by CGCM3. Among six global model-regional model pairs, HRM3 driven by GFDL generally shows strong decreases in frequency across two analyses and two periods, while strong increases are consistently observed for MM5I driven by CCSM. The resulting model medians do not present evident and consistent trends across two analyses and periods, unlike the CMIP5 counterparts. The medians of precipitation and analogue suggest 0.1 and 1.1 fewer events per year during the 1st period but 0.9 and 0.2 more events per year during the 2nd period, respectively. The inter-model spread in the projected changes remains fairly large for the ensemble of NARCCAP model precipitation, from a decrease of 5 to an increase of 6 events, comparable to that of the CMIP5 model precipitation. Analogue scheme significantly reduces the inter-model discrepancies, especially during the 1st period. Overall, except for the HRM3 driven by GFDL, the consistencies in the sign of change between GCM-driven RCMs and corresponding CMIP5 models are poor, which is likely attributed to RCMs' high sensitivity to the choice in physical parameterizations. Frequency changes from the analogue scheme $uvw_{500}q_{2m}$ illustrates very similar features to those from $uvw_{500}tpw$, except that both multi-model medians and individual model of $uvw_{500}q_{2m}$ demonstrate stronger drying trends (**Figure 4b**). This is true for both CMIP5 and NARCCAP results with their multi-model medians indicating 2.3–3.2 (*CMP_A_*) and 1.4 (*NAR_A_*) fewer events per year, respectively. Likewise, the analogue scheme significantly reduces the inter-model discrepancies in comparison with the CMIP5 or NARCCAP model precipitation counterpart.

One caveat of our study is that we only address the uncertainty in projections from inter-model differences in representing physical processes, but not internal (natural) climate system variability. This contributes to uncertainty in climate change projections and influences interpretation of climate trends. Hawkins and Sutton (2009, 2011) suggest that the internal climate system variability is likely to be the dominant source of uncertainty in precipitation change in the near term over North America, while model structure uncertainty will dominate in the medium to long term. Based on a 40-member physically uniform ensemble, Deser *et al.* (2012) illustrated substantial natural variability in mid-21st century precipitation projections in large parts of the US. Sriver *et al.* (2015) demonstrated that 34 CMIP5 models yield a considerably larger spread in representing local-scale daily summer precipitation maxima than the 50 Community Earth System Model (CESM) ensemble simulations with different initial conditions. Singh *et al.* (2013) compared the five-member CCSM3-RegCM3 ensemble spread in projections of various annual precipitation metrics with the 10-member NARCCAP ensemble spread in the mid-century period. They found the inter-model spread dominates for the simulated frequency of extreme wet events and average intensity in most regions of the U.S., but is comparable to the intra-ensemble spread for extreme event intensity and total precipitation. These studies suggest that the relative contribution of internal variability and model structural differences depends on the variable and period of interest, and cautions should be taken for an interpretation of the projected trends—particularly those based on smaller ensembles.

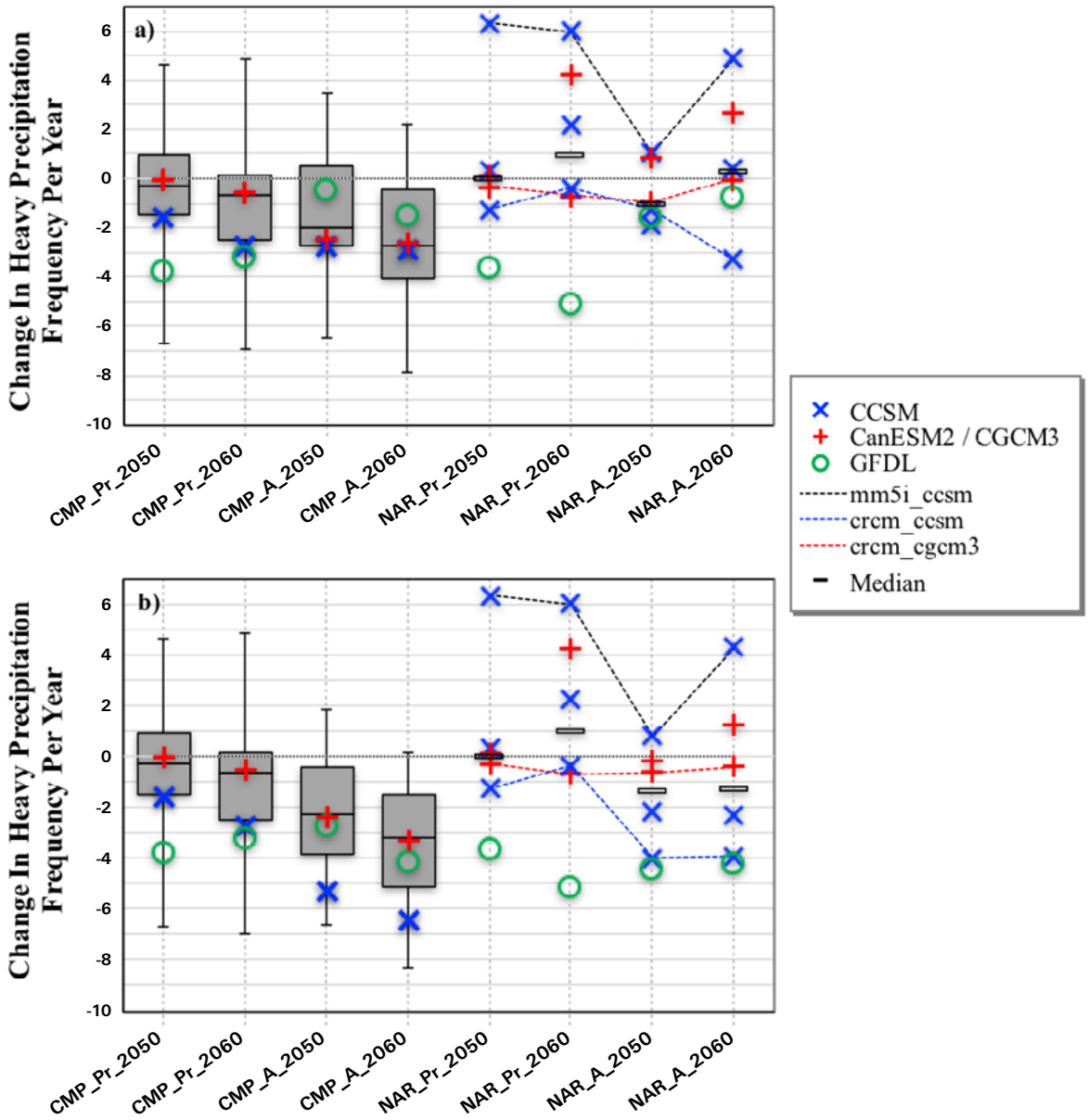

Figure 4. a) The changes in heavy precipitation frequency estimated from an ensemble of CMIP5 (*CMP_Pr_*) model precipitation and the analogue scheme $uvw_{500}tpw$ (*CMP_A_*) under the RCP8.5 scenario (whisker bars) as well as the counterparts from an ensemble of NARCCAP RCMs (*NAR_Pr_* and *NAR_A_*) under the SRESA2 scenario (scatters) during the periods centered at 2050 (2041-2059) and 2060 (2051-2069), respectively. b) Same as a) but for the analogue scheme $uvw_{500}q_{2m}$. Selected NARCCAP ensembles (lines) are labeled to differentiate from other.

4. Summary and Discussion

Precipitation is generally not well simulated in global climate models because it is influenced by vertical motions and orography on scales smaller than the model grid. Regional climate models are often perceived as an optimum approach to achieve better resolution of these high detail features, which are assumed to help produce heavy precipitation statistics that are closer to reality than the coarse-resolution global climate models. One alternative is an analogue style of statistical downscaling, which identifies the synoptic atmospheric circulation conditions that are well-resolved in climate models to derive such statistics at the regional scale. In this study, we investigate the abilities of RCMs and GCMs, when regridded to a common GCM-scale grid, to quantify the present-day summer heavy precipitation frequency and future changes in the Midwestern U.S. (MWST) based on model-simulated precipitation *versus* an analogue method.

We examine two analogue schemes constructed with the combinations of atmospheric circulation variables (500 hPa horizontal and vertical wind vectors) and different water vapor content variables (near-surface specific humidity and column precipitable water). The analogue schemes are first calibrated with 19-yr (1980–1998) and

then validated with 16-yr (1999–2014) MERRA-2 reanalysis. We found that the performances of two analogue schemes are comparable to those of MERRA-2 assimilated precipitation and MERRA-2 bias-corrected precipitation in characterizing the occurrence and interannual variations of observed heavy precipitation events in the MWST. They all significantly improve upon MERRA assimilated precipitation, which considerably underestimates the number of heavy precipitation events in MWST.

17 out of 18 CMIP5 models and all 6 GCM driven NARCCAP ensemble underestimate the late twentieth-century (1980–1998) summer heavy precipitation frequencies with considerably large inter-model spreads, revealing the wide variation in both GCMs' and RCMs' abilities to reproduce the heavy precipitation over the MWST. The comparable inter-model spread exhibited by the six GCM-RCM pairs to that of 18 CMIP5 GCMs further highlights the strong sensitivity of RCM to the physical parameterizations that are chosen, as pointed out in several studies (Hewitson and Crane, 2006; Christensen *et al.*, 2007). However, RCMs generally improve upon the corresponding driving models from CMIP5, indicating that the better represented characteristics of RCM-simulated precipitation at the native grid (50km) can be preserved to some extent after being regridded to the coarse resolution (2.5°×2°). In contrast, regardless of the atmospheric synoptic conditions chosen from the coarse resolution GCMs or the regridded RCMs, the analogue schemes greatly improve upon their model precipitation counterparts in terms of the assessment of heavy precipitation frequency from the perspectives of both accuracy (consistencies with observation) and precision (inter-model spreads). Unlike model precipitation, the analogue schemes based on CMIP5 models perform better than those based on RCMs, which is probably attributed to the improved model components adopted in the CMIP5 GCMs compared to those in the NARCCAP driving GCMs.

The multimodel medians of both model precipitation and analogue schemes based on CMIP5 indicate decreases in heavy precipitation frequency by the middle of this century in absence of climate change policies, with the drying trends of the analogue results stronger than those of precipitation. Both analyses exhibit large uncertainty in the sign and magnitude of change. The GCM driven RCMs show very mixed responses and the resulting multimodel medians do not present consistent trends across model precipitation and analogue schemes. Note our study only considers a small number (4) of RCMs with their lateral boundary conditions provided from small number (3) of global models. The limited NARCCAP ensemble is not sufficient to definitely sample the full range of uncertainty, which stems not only from the differences in RCM's parameterization schemes but also from the representation of the large-scale driving hydrodynamics from GCMs. Nevertheless, we find that the analogue schemes based on both CMIP5 and regridded RCMs outperform their model precipitation counterparts with considerably reduced inter-model spread.

Feser *et al.* (2011) reviewed the RCMs' potential added value to global models and found that improvements depend essentially on the kind of application, experiment setup, analyzed model variable, and location. Di Luca (2011) also examined a necessary condition for the RCM technique to generate some added value. Both studies concluded that regional models showed an added value if the climate statistics of interest contain some fine spatial-scale variability (i.e. mesoscale phenomena, orography, coastlines) that would be absent on a coarser grid. This is consistent with what our results indicate. Model-simulated precipitation regridded from the RCMs improves upon that from the corresponding driving GCMs in estimating heavy precipitation frequency (i.e. Figure 3) because summertime local precipitation extremes depend strongly on small-scale atmospheric features (i.e. convective cells) that are best resolved by the regional model. On the other hand, the analogue method demonstrates a weak potential to improve the NARCCAP skill over its GCM driver because the method relies on the synoptic atmospheric conditions that are well described in global model data and thus the higher spatial resolution is less important. In summary, a RCM is essential for assessing the potential impacts of local forcing (e.g. topography, land-water boundaries, land use and land cover change). However, its high sensitivity to the chosen physical parameterizations will also influence its ability to add value. The analogue method presented here, given its weaker dependence on resolution, the convergence in the circulation response among GCMs, and the continued improvement in climate model physics, offers a robust but economic way of assessing heavy precipitation frequency across a broad range of GCMs and multiple climate change scenarios, which could be extremely useful from the policy and planning perspective.

Acknowledgements

This work was funded by MacroSystems Biology Program Grant (NSF-AES EF#1137306) from National Science Foundation and An Integrated Framework for Climate Change Assessment (DE-FG02-94ER61937) from the Department of Energy. We acknowledge the modeling groups, the Program for Climate Model Diagnosis and Intercomparison (PCMDI), and the WCRP's Working Group on Coupled Modeling (WGCM) for their roles in making available the WCRP CMIP5 multimodel dataset. We also thank the North American Regional Climate Change Assessment Program (NARCCAP) for providing the data used in this paper, the NOAA Climate Prediction Center for the global gridded precipitation observations, and the NASA Global Modeling and Assimilation Office for the MERRA-2 Reanalysis data.

5. References

Bosilovich, M. G., R. Lucchesi & M. Suarez, 2016: MERRA-2: File Specification. GMAO Office Note No. 9 (Version 1.1), 73 pp, available from http://gmao.gsfc.nasa.gov/pubs/office_notes.

Chen, C. & T. Knutson, 2008: On the verification and comparison of extreme rainfall indices from climate models. *J. Clim.*, **21**: 1605–1621.

Christensen, J. & Coauthors, 2007: Prediction of regional scenarios and uncertainties for defining European climate change risks and effects: The Prudence project. *Climatic Change,* **81:** 1–371.

Chylek, P., J. Li, M.K. Dubey, M. Wang & G. Lesins, 2011: Observed and model simulated 20th century Arctic temperature variability: Canadian Earth System Model CanESM2. *Atmos. Chem. Phys. Discuss.*, **11**: 22893–22907.

Collins, W.D., C.M. Bitz, M.L. Blackmon, G.B. Bonan, C.S. Bretherton, J.A. Carton, P. Chang, S.C. Doney, J.J. Hack, T.B. Henderson, J.T. Kiehl, W.G. Large, D.S. McKenna, B.D. Santer & R.D. Smith, 2006: The community climate system model Version 3 (CCSM3). *J. Clim.*, **19**: 2122–2143.

Covey, C., K.M. AchutaRao, S.J. Lambert & K.E. Taylor, 2000: Intercomparison of Present and Future Climates Simulated by Coupled Ocean–Atmosphere GCMs, Program for Climate Model Diagnosis and Intercomparison Report #66, Lawrence Livermore National Laboratory UCRL-ID-140325

Dai, A., 2006: Precipitation characteristics in eighteen coupled climate models. *J. Clim.*, **19**: 4605–4630.

DeAngelis, A.M., A.J. Broccoli & S.G. Decker, 2013: A comparison of CMIP3 simulations of precipitation over North America with observations: Daily statistics and circulation features accompanying extreme events. *J. Clim.*, **26**: 3209– 3230.

Delworth, T. *et al.*, 2006: GFDL's CM2 global coupled climate models—Part 1: formulation and simulation characteristics. *J. Clim.*, **19**: 643–674.

Deser, C., R. Knutti, S. Solomon & A. S. Phillips, 2012: Communication of the role of natural variability in future North American climate, *Nat. Clim. Change*, **2**: 775–779.

Di Luca, A., R. de Elia, R. Laprise, 2011: Potential for added value in precipitation simulated by high-resolution nested Regional Climate Models and observations. *Clim. Dyn.,* **38**: 1229–1247.

Donner, L.J. & Coauthors, 2011: The dynamical core, physical parameterizations, and basic simulation characteristics of the atmospheric component AM3 of the GFDL Global Coupled Model CM3. *J. Clim.*, **24**: 3484–3519.

Duffy, P.B., B. Govindasamy, J.P. Lorio, J. Milovich, K.R. Sperber, K.E. Taylor, M.F. Wehner & S.L. Thompson, 2003: High-resolution simulations of global climate, Part 1: Present climate, *Clim. Dyn.*, **21**: 371–390.

Feser, F., B. Rockel, H. von Storch, J. Winterfeldt & M. Zahn, 2011: Regional Climate Models Add Value to Global Model Data: A Review and Selected Examples. *Bull. Amer. Meteor. Soc.,* **92**: 1181–1192.

Flato, G.M., G.J. Boer, W.G. Lee, N.A. McFarlane, D. Ramsden, M.C. Reader & A.J. Weaver, 2000: The Canadian center for climate modeling and analysis global coupled model and its climate. *Clim. Dyn.*, **16**: 451–467.

Frei, C., R. Scholl, S. Fukutome, J. Schmidli & P.L. Vidale, 2006: Future change of precipitation extremes in Europe: intercomparison of scenarios from regional climate models. *J. Geophys. Res.*, **111**, D06105, doi:10.1029/2005JD005965.

Gao, X., C.A. Schlosser, P. Xie, E. Monier & D. Entekhabi, 2014: An Analogue Approach to Identify Heavy Precipitation Events: Evaluation and Application to CMIP5 Climate Models in the United States. *J. Climate,* **27**: 5941–5963.

Gao, X., C. A. Schlosser, P.A. O'Gorman, E. Monier & D. Entekhabi, 2017: Twenty-First-Century Changes in U.S. Regional Heavy Precipitation Frequency Based on Resolved Atmospheric Patterns. *J. Climate,* **30**: 2501–2521.

Gent, P.R., 2011: The Community Climate System Model Version 4. *J. Clim.*, **24**: 4973–4991.

Grell, G.A. & D. Devenyi, 2002: A generalized approach to parameterizing convection combining ensemble and data assimilation techniques. *Geophys. Res. Lett.*, **29**: 1693–1697.

Grell, G., J. Dudhia & D. Stauffer, 1995: A description of the Fifth-Generation Penn State/NCAR Mesoscale Model (MM5) NCAR Technical Note, NCAR/TN-398 + STR

Griffies, S.M., M. Winton, L.J. Donner, L.W. Horowitz, S.M. Downes, R. Farneti, A. Gnanadesikan, W.J. Hurlin, H. Lee, Z. Liang, J.B. Palter, B.L. Samuels, A.T. Wittenberg, B.L. Wyman, J. Yin & N. Zadeh, 2011: The GFDL CM3 Coupled Climate Model: Characteristics of the Ocean and Sea Ice Simulations. *J. Climate,* **24**: 3520–3544.

Grotjahn, R., 2011: Identifying extreme hottest days from large scale upper air data: A pilot scheme to find California Central Valley summertime maximum surface temperatures. *Clim. Dyn.*, **37**: 587–604.

Gutowski, W.J., Jr., S.S. Willis, J.C. Patton, B.R.J. Schwedler, R.W. Arritt & E.S. Takle, 2008: Changes in extreme, cold-season synoptic precipitation events under global warming. *Geophys. Res. Lett.*, **35**, L20710, doi:10.1029/2008GL035516.

Hawkins, E. & R. Sutton, 2009: The potential to narrow uncertainty in regional climate predictions. *Bull. Am. Meteorol. Soc.*, **90**: 1095–1107.

Hawkins, E. & R. Sutton, 2011: The potential to narrow uncertainty in projections of regional precipitation change. *Clim. Dyn.*, **37**: 407–418.

Hewitson, B.C. & R.G. Crane, 2006: Consensus between GCM climate change projections with empirical downscaling: Precipitation downscaling over South Africa. *Int. J. Climatol.*, **26**: 1315–1337.

Higgins, R.W., W. Shi, E. Yarosh & R. Joyce, 2000: Improved US Precipitation Quality Control System and Analysis. NCEP/ Climate Prediction Center ATLAS No. 7, National Centers for Environmental Prediction, Climate Prediction Center, Camp Springs, Maryland. Available at http://www.cpc.ncep.noaa. gov/ research_papers/ncep_cpc_atlas/7/index.html. Data is available at http://www.cdc.noaa.gov/cdc/data.unified.html

Iorio, J.P., P.B. Duffy, B. Govindasamy, S.L. Thompson, M. Khairoutdinov & D. Randall, 2004: Effects of model resolution and subgrid-scale physics on the simulation of precipitation in the continental United States. *Clim. Dyn.*, **23**: 243–258.

Jones, R., M. Noguer, D. Hassell, D. Hudson, S. Wilson, G. Jenkins & J. Mitchell, 2004: Generating high resolution climate change scenarios using PRECIS. Met Office Hadley Centre, Exeter, p40.

Kawazoe, S. & W.J. Gutowski, 2013: Regional, very heavy daily precipitation in NARCCAP simulations. *J. Hydrometeor.,* **14**: 1212–1227.

Kharin, V.V., F.W. Zwiers, X. Zhang & G.C. Hegerl, 2007: Changes in temperature and precipitation extremes in the IPCC ensemble of global coupled model simulations. *J. Clim.*, **20**: 1419–1444.

Li, F., W.D. Collins, M.F. Wehner, D.L. Williamson, J.G. Olson & C. Algieri, 2011: Impact of horizontal resolution on simulation of precipitation extremes in an aqua-planet version of Community Atmospheric Model (CAM3). *Tellus A*, **63**: 884–892.

Mearns, L.O., W.J. Gutowski, R. Jones, L.Y. Leung, S. McGinnis, A.M.B. Nunes & Y. Qian, 2009: A regional climate change assessment program for North America. *EOS*, **90**: 311–312.

Molod, A., L. Takacs, M. Suarez & J. Bacmeister, 2015: Development of the GEOS-5 atmospheric general circulation model: evolution from MERRA to MERRA2. *Geosci. Model Dev.*, **8**: 1339–1356.

Meehl, G.A., C. Covey, K.E. Taylor, T. Delworth, R.J. Stouffer, M. Latif, B. McAvaney & J.F. Mitchell, 2007: The WCRP CMIP3 multimodel dataset: A new era in climate change research. *Bull. Amer. Meteor. Soc.,* **88**: 1383–1394.

Music, B. & D. Caya, 2007: Evaluation of the hydrological cycle over the Mississippi River Basin as simulated by the Canadian regional climate model (CRCM). *J. Hydrometeor*, **8**: 969–988.

Nakićenović, N. & R. Swart, 2000: Special report on emissions scenarios: a special report of Working Group III on the Intergovernmental Panel on Climate Change. Cambridge University Press, Cambridge

Oouchi, K., J. Yoshimura, H. Yoshimura, R. Mizuta, S. Kusunoki & A. Noda, 2006: Tropical cyclone climatology in a global-warming climate as simulated in a 20 km-mesh global atmospheric model: frequency and wind intensity analysis. *J. Meteorol. Soc. Japan.*, **84**: 259–276.

Reichle, R., Q. Liu, R. Koster, C. Draper, S. Mahanama & G. Partyka, 2017. Land Surface Precipitation in MERRA-2. *J. Clim.*, **30**: 1643–1664.

Singh, D., M. Tsiang, B. Rajaratnam & N. S. Diffenbaugh, 2013: Precipitation extremes over the continental United States in a transient, high-resolution, ensemble climate model experiment, *J. Geophys. Res. Atmos.,* **118**: 7063–7086.

Skamarock, W.C., J.B. Klemp, J. Dudhia, D.O. Gill, D.M. Barker, W. Wang & J.G. Powers, 2005: A description of the advanced research WRF Version 2. NCAR Tech Notes-468+STR (http://www.mmm.ucar.edu/wrf/users/docs/arw_v2.pdf)

Sriver, R. L., C. E. Forest & K. Keller, 2015: Effects of initial conditions uncertainty on regional climate variability: An analysis using a low-resolution CESM ensemble. *Geophys. Res. Lett.*, **42**: 5468–5476.

Sun, Y., S. Solomon, A. Dai & R. W. Portmann, 2006: How often does it rain? *J. Clim.*, **19**: 916–934.

Taylor, K. E., R.J. Stouffer & G.A. Meehl, 2012: An overview of CMIP5 and the experiment design. *Bull. Amer. Meteor. Soc.*, **93**: 485– 498.

Wehner, M.F., R. Smith, P. Duffy & G. Bala, 2010: The effect of horizontal resolution on simulation of very extreme US precipitation events in a global atmosphere model. *Clim. Dyn.*, **32**: 241–247.

Wehner, M.F., 2013: Very extreme seasonal precipitation in the NARCCAP ensemble: model performance and projections. *Clim. Dyn.*, **40**: 59–80.

Joint Program Report Series - Recent Articles

For limited quantities, Joint Program Reports are available free of charge. Contact the Joint Program Office to order.
Complete list: http://globalchange.mit.edu/publications

322. **Mid-Western U.S. Heavy Summer-Precipitation in Regional and Global Climate Models: The Impact on Model Skill and Consensus Through an Analogue Lens.** *Gao and Schlosser, Oct 2017*
321. **New data for representing irrigated agriculture in economy-wide models.** *Ledvina et al., Oct 2017*
320. **Probabilistic projections of the future climate for the world and the continental USA.** *Sokolov et al., Sep 2017*
319. **Estimating the potential of U.S. urban infrastructure albedo enhancement as climate mitigation in the face of climate variability.** *Xu et al., Sep 2017*
318. **A Win-Win Solution to Abate Aviation CO_2 emissions.** *Winchester, Aug 2017*
317. **Application of the Analogue Method to Modeling Heat Waves: A Case Study With Power Transformers.** *Gao et al., Aug 2017*
316. **The Revenue Implications of a Carbon Tax.** *Yuan et al., Jul 2017*
315. **The Future Water Risks Under Global Change in Southern and Eastern Asia: Implications of Mitigation.** *Gao et al., Jul 2017*
314. **Modeling the Income Dependence of Household Energy Consumption and its Implications for Climate Policy in China.** *Caron et al., Jul 2017*
313. **Global economic growth and agricultural land conversion under uncertain productivity improvements in agriculture.** *Lanz et al., Jun 2017*
312. **Can Tariffs be Used to Enforce Paris Climate Commitments?** *Winchester, Jun 2017*
311. **A Review of and Perspectives on Global Change Modeling for Northern Eurasia.** *Monier et al., May 2017*
310. **The Future of Coal in China.** *Zhang et al., Apr 2017*
309. **Climate Stabilization at 2°C and Net Zero Carbon Emissions.** *Sokolov et al., Mar 2017*
308. **Transparency in the Paris Agreement.** *Jacoby et al., Feb 2017*
307. **Economic Projection with Non-homothetic Preferences: The Performance and Application of a CDE Demand System.** *Chen, Dec 2016*
306. **A Drought Indicator based on Ecosystem Responses to Water Availability: The Normalized Ecosystem Drought Index.** *Chang et al., Nov 2016*
305. **Is Current Irrigation Sustainable in the United States? An Integrated Assessment of Climate Change Impact on Water Resources and Irrigated Crop Yields.** *Blanc et al., Nov 2016*
304. **The Impact of Oil Prices on Bioenergy, Emissions and Land Use.** *Winchester & Ledvina, Oct 2016*
303. **Scaling Compliance with Coverage? Firm-level Performance in China's Industrial Energy Conservation Program.** *Karplus et al., Oct 2016*
302. **21st Century Changes in U.S. Heavy Precipitation Frequency Based on Resolved Atmospheric Patterns.** *Gao et al., Oct 2016*
301. **Combining Price and Quantity Controls under Partitioned Environmental Regulation.** *Abrell & Rausch, Jul 2016*
300. **The Impact of Water Scarcity on Food, Bioenergy and Deforestation.** *Winchester et al., Jul 2016*
299. **The Impact of Coordinated Policies on Air Pollution Emissions from Road Transportation in China.** *Kishimoto et al., Jun 2016*
298. **Modeling Regional Carbon Dioxide Flux over California using the WRF-ACASA Coupled Model.** *Xu et al., Jun 2016*
297. **Electricity Investments under Technology Cost Uncertainty and Stochastic Technological Learning.** *Morris et al., May 2016*
296. **Statistical Emulators of Maize, Rice, Soybean and Wheat Yields from Global Gridded Crop Models.** *Blanc, May 2016*
295. **Are Land-use Emissions Scalable with Increasing Corn Ethanol Mandates in the United States?** *Ejaz et al., Apr 2016*
294. **The Future of Natural Gas in China: Effects of Pricing Reform and Climate Policy.** *Zhang & Paltsev, Mar 2016*
293. **Uncertainty in Future Agro-Climate Projections in the United States and Benefits of Greenhouse Gas Mitigation.** *Monier et al., Mar 2016*
292. **Costs of Climate Mitigation Policies.** *Chen et al., Mar 2016*
291. **Scenarios of Global Change: Integrated Assessment of Climate Impacts.** *Paltsev et al., Feb 2016*
290. **Modeling Uncertainty in Climate Change: A Multi-Model Comparison.** *Gillingham et al., Dec 2015*
289. **The Impact of Climate Policy on Carbon Capture and Storage Deployment in China.** *Zhang et al., Dec 2015*
288. **The Influence of Gas-to-Liquids and Natural Gas Production Technology Penetration on the Crude Oil-Natural Gas Price Relationship.** *Ramberg et al., Dec 2015*
287. **Impact of Canopy Representations on Regional Modeling of Evapotranspiration using the WRF-ACASA Coupled Model.** *Xu et al., Dec 2015*
286. **Launching a New Climate Regime.** *Jacoby & Chen, Nov 2015*

MIT Joint Program on the Science and Policy of Global Change

Massachusetts Institute of Technology
77 Massachusetts Ave., E19-411
Cambridge MA 02139-4307 (USA)

T (617) 253-7492 **F** (617) 253-9845
globalchange@mit.edu
http://globalchange.mit.edu/